UNIVERSITY OF AMSTERDAM

UvA-DARE (Digital Academic Repository)

Discovery of the Hard Spectrum VHE γ-Ray Source HESS J1641-463

Abramowski, A.; et al., [Unknown]; Balzer, A.; Berge, D.; Bryan, M.; Salek, D.; Vink, J.

DOI
10.1088/2041-8205/794/1/L1

Publication date
2014

Document Version
Final published version

Published in
Astrophysical Journal Letters

Link to publication

Citation for published version (APA):
Abramowski, A., et al., U., Balzer, A., Berge, D., Bryan, M., Salek, D., & Vink, J. (2014). Discovery of the Hard Spectrum VHE γ-Ray Source HESS J1641-463. *Astrophysical Journal Letters*, *794*(1), L1. https://doi.org/10.1088/2041-8205/794/1/L1

General rights
It is not permitted to download or to forward/distribute the text or part of it without the consent of the author(s) and/or copyright holder(s), other than for strictly personal, individual use, unless the work is under an open content license (like Creative Commons).

Disclaimer/Complaints regulations
If you believe that digital publication of certain material infringes any of your rights or (privacy) interests, please let the Library know, stating your reasons. In case of a legitimate complaint, the Library will make the material inaccessible and/or remove it from the website. Please Ask the Library: https://uba.uva.nl/en/contact, or a letter to: Library of the University of Amsterdam, Secretariat, P.O. Box 19185, 1000 GD Amsterdam, The Netherlands. You will be contacted as soon as possible.

UvA-DARE is a service provided by the library of the University of Amsterdam (https://dare.uva.nl)

Download date:10 Oct 2026

The Astrophysical Journal Letters, 794:L1 (6pp), 2014 October 10 doi:10.1088/2041-8205/794/1/L1
© 2014. The American Astronomical Society. All rights reserved. Printed in the U.S.A.

DISCOVERY OF THE HARD SPECTRUM VHE γ-RAY SOURCE HESS J1641−463

A. Abramowski[1], F. Aharonian[2,3,4], F. Ait Benkhali[2], A. G. Akhperjanian[4,5], E. O. Angüner[6], M. Backes[7], S. Balenderan[8], A. Balzer[9], A. Barnacka[10,41], Y. Becherini[11], J. Becker Tjus[12], D. Berge[13], S. Bernhard[14], K. Bernlöhr[2,6], E. Birsin[6], J. Biteau[15,42], M. Böttcher[16], C. Boisson[17], J. Bolmont[18], P. Bordas[19], J. Bregeon[20], F. Brun[21], P. Brun[21], M. Bryan[9], T. Bulik[22], S. Carrigan[2], S. Casanova[2,23], P. M. Chadwick[8], N. Chakraborty[2], R. Chalme-Calvet[18], R. C. G. Chaves[20], M. Chrétien[18], S. Colafrancesco[24], G. Cologna[25], J. Conrad[26,43], C. Couturier[18], Y. Cui[19], M. Dalton[27], I. D. Davids[7,16], B. Degrange[15], C. Deil[2], P. deWilt[28], A. Djannati-Ataï[29], W. Domainko[2], A. Donath[2], L. O'C. Drury[3], G. Dubus[30], K. Dutson[31], J. Dyks[32], M. Dyrda[23], T. Edwards[2], K. Egberts[33], P. Eger[2], P. Espigat[29], C. Farnier[26], S. Fegan[15], F. Feinstein[20], M. V. Fernandes[1], D. Fernandez[20], A. Fiasson[34], G. Fontaine[15], A. Förster[2], M. Füßling[33], S. Gabici[29], M. Gajdus[6], Y. A. Gallant[20], T. Garrigoux[18], G. Giavitto[35], B. Giebels[15], J. F. Glicenstein[21], D. Gottschall[19], M.-H. Grondin[27], M. Grudzińska[22], D. Hadasch[14], S. Häffner[36], J. Hahn[2], J. Harris[8], G. Heinzelmann[1], G. Henri[30], G. Hermann[2], O. Hervet[17], A. Hillert[2], J. A. Hinton[31], W. Hofmann[2], P. Hofverberg[2], M. Holler[33], D. Horns[1], A. Ivascenko[16], A. Jacholkowska[18], C. Jahn[36], M. Jamrozy[10], M. Janiak[32], F. Jankowsky[25], I. Jung-Richardt[36], M. A. Kastendieck[1], K. Katarzyński[37], U. Katz[36], S. Kaufmann[25], B. Khélifi[29], M. Kieffer[18], S. Klepser[35], D. Klochkov[19], W. Kluźniak[32], D. Kolitzus[14], Nu. Komin[24], K. Kosack[21], S. Krakau[12], F. Krayzel[34], P. P. Krüger[16], H. Laffon[27], G. Lamanna[34], J. Lau[28], J. Lefaucheur[29], V. Lefranc[21], A. Lemière[29], M. Lemoine-Goumard[27], J.-P. Lenain[18], T. Lohse[6], A. Lopatin[36], C.-C. Lu[2], V. Marandon[2], A. Marcowith[20], R. Marx[2], G. Maurin[34], N. Maxted[20], M. Mayer[33], T. J. L. McComb[8], J. Méhault[27], P. J. Meintjes[38], U. Menzler[12], M. Meyer[26], A. M. W. Mitchell[2], R. Moderski[32], M. Mohamed[25], K. Morå[26], E. Moulin[21], T. Murach[6], M. de Naurois[15], J. Niemiec[23], S. J. Nolan[8], L. Oakes[6], H. Odaka[2], S. Ohm[35], B. Opitz[1], M. Ostrowski[10], I. Oya[35], M. Panter[2], R. D. Parsons[2], M. Paz Arribas[6], N. W. Pekeur[16], G. Pelletier[30], P.-O. Petrucci[30], B. Peyaud[21], S. Pita[29], H. Poon[2], G. Pühlhofer[19], M. Punch[29], A. Quirrenbach[25], S. Raab[36], I. Reichardt[29], A. Reimer[14], O. Reimer[14], M. Renaud[20], R. de los Reyes[2], F. Rieger[2], C. Romoli[3], S. Rosier-Lees[34], G. Rowell[28], B. Rudak[32], C. B. Rulten[17], V. Sahakian[4,5], D. Salek[39], D. A. Sanchez[34], A. Santangelo[19], R. Schlickeiser[12], F. Schüssler[21], A. Schulz[35], U. Schwanke[6], S. Schwarzburg[19], S. Schwemmer[25], H. Sol[17], F. Spanier[16], G. Spengler[26], F. Spies[1], Ł. Stawarz[10], R. Steenkamp[7], C. Stegmann[33,35], F. Stinzing[36], K. Stycz[35], I. Sushch[6,16], J.-P. Tavernet[18], T. Tavernier[29], A. M. Taylor[3], R. Terrier[29], M. Tluczykont[1], C. Trichard[34], K. Valerius[36], C. van Eldik[36], B. van Soelen[38], G. Vasileiadis[20], J. Veh[36], C. Venter[16], A. Viana[2], P. Vincent[18], J. Vink[9], H. J. Völk[2], F. Volpe[2], M. Vorster[16], T. Vuillaume[30], S. J. Wagner[25], P. Wagner[6], R. M. Wagner[26], M. Ward[8], M. Weidinger[12], Q. Weitzel[2], R. White[31], A. Wierzcholska[23], P. Willmann[36], A. Wörnlein[36], D. Wouters[21], R. Yang[2], V. Zabalza[2,31], D. Zaborov[15], M. Zacharias[25], A. A. Zdziarski[32], A. Zech[17], H.-S. Zechlin[1], Y. Fukui[40], H. Sano[40], T. Fukuda[40], and S. Yoshiike[40]
(H.E.S.S. Collaboration)

[1] Institut für Experimentalphysik, Universität Hamburg, Luruper Chaussee 149, D-22761 Hamburg, Germany
[2] Max-Planck-Institut für Kernphysik, PO Box 103980, D-69029 Heidelberg, Germany; sabrina.casanova@ifj.edu.pl, sabrina.casanova@mpi-hd.mpg.de
[3] Dublin Institute for Advanced Studies, 31 Fitzwilliam Place, Dublin 2, Ireland
[4] National Academy of Sciences of the Republic of Armenia, Marshall Baghramian Avenue, 24, 0019 Yerevan, Republic of Armenia
[5] Yerevan Physics Institute, 2 Alikhanian Brothers Street, 375036 Yerevan, Armenia
[6] Institut für Physik, Humboldt-Universität zu Berlin, Newtonstr. 15, D-12489 Berlin, Germany
[7] Department of Physics, University of Namibia, Private Bag 13301, Windhoek, Namibia
[8] Department of Physics, University of Durham, South Road, Durham DH1 3LE, UK
[9] GRAPPA, Anton Pannekoek Institute for Astronomy, University of Amsterdam, Science Park 904, 1098 XH Amsterdam, The Netherlands
[10] Obserwatorium Astronomiczne, Uniwersytet Jagielloński, ul. Orla 171, 30-244 Kraków, Poland
[11] Department of Physics and Electrical Engineering, Linnaeus University, 351 95 Växjö, Sweden
[12] Institut für Theoretische Physik, Lehrstuhl IV: Weltraum und Astrophysik, Ruhr-Universität Bochum, D-44780 Bochum, Germany
[13] GRAPPA, Anton Pannekoek Institute for Astronomy and Institute of High-Energy Physics, University of Amsterdam, Science Park 904, 1098 XH Amsterdam, The Netherlands
[14] Institut für Astro- und Teilchenphysik, Leopold-Franzens-Universität Innsbruck, A-6020 Innsbruck, Austria
[15] Laboratoire Leprince-Ringuet, Ecole Polytechnique, CNRS/IN2P3, F-91128 Palaiseau, France
[16] Centre for Space Research, North-West University, Potchefstroom 2520, South Africa
[17] LUTH, Observatoire de Paris, CNRS, Université Paris Diderot, 5 Place Jules Janssen, F-92190 Meudon, France
[18] LPNHE, Université Pierre et Marie Curie Paris 6, Université Denis Diderot Paris 7, CNRS/IN2P3, 4 Place Jussieu, F-75252, Paris Cedex 5, France
[19] Institut für Astronomie und Astrophysik, Universität Tübingen, Sand 1, D-72076 Tübingen, Germany
[20] Laboratoire Univers et Particules de Montpellier, Université Montpellier 2, CNRS/IN2P3, CC 72, Place Eugène Bataillon, F-34095 Montpellier Cedex 5, France
[21] DSM/Irfu, CEA Saclay, F-91191 Gif-Sur-Yvette Cedex, France
[22] Astronomical Observatory, The University of Warsaw, Al. Ujazdowskie 4, 00-478 Warsaw, Poland
[23] Instytut Fizyki Jądrowej PAN, ul. Radzikowskiego 152, 31-342 Kraków, Poland
[24] School of Physics, University of the Witwatersrand, 1 Jan Smuts Avenue, Braamfontein, Johannesburg 2050, South Africa
[25] Landessternwarte, Universität Heidelberg, Königstuhl, D-69117 Heidelberg, Germany
[26] Oskar Klein Centre, Department of Physics, Stockholm University, Albanova University Center, SE-10691 Stockholm, Sweden
[27] Centre d'Études Nucléaires de Bordeaux Gradignan, Université Bordeaux 1, CNRS/IN2P3, F-33175 Gradignan, France
[28] School of Chemistry & Physics, University of Adelaide, Adelaide 5005, Australia

[29] APC, AstroParticule et Cosmologie, Université Paris Diderot, CNRS/IN2P3, CEA/Irfu, Observatoire de Paris, Sorbonne Paris Cité, 10, rue Alice Domon et Léonie Duquet, F-75205 Paris Cedex 13, France
[30] CNRS, Univ. Grenoble Alpes, IPAG, F-38000 Grenoble, France IPAG, F-38000 Grenoble, France
[31] Department of Physics and Astronomy, The University of Leicester, University Road, Leicester, LE1 7RH, UK
[32] Nicolaus Copernicus Astronomical Center, ul. Bartycka 18, 00-716 Warsaw, Poland
[33] Institut für Physik und Astronomie, Universität Potsdam, Karl-Liebknecht-Strasse 24/25, D-14476 Potsdam, Germany
[34] Laboratoire d'Annecy-le-Vieux de Physique des Particules, Université de Savoie, CNRS/IN2P3, F-74941 Annecy-le-Vieux, France
[35] DESY, D-15738 Zeuthen, Germany; igor.oya.vallejo@desy.de
[36] Physikalisches Institut, Universität Erlangen-Nürnberg, Erwin-Rommel-Str. 1, D-91058 Erlangen, Germany
[37] Centre for Astronomy, Faculty of Physics, Astronomy and Informatics, Nicolaus Copernicus University, Grudziadzka 5, 87-100 Torun, Poland
[38] Department of Physics, University of the Free State, PO Box 339, Bloemfontein 9300, South Africa
[39] GRAPPA, Institute of High-Energy Physics, University of Amsterdam, Science Park 904, 1098 XH Amsterdam, The Netherlands
[40] Department of Physics, Nagoya University, Furo-cho, Chiku sa-ku, Nagoya, 464-8601, Japan
Received 2014 August 21; accepted 2014 September 6; published 2014 September 22

ABSTRACT

This Letter reports the discovery of a remarkably hard spectrum source, HESS J1641−463, by the High Energy Stereoscopic System (H.E.S.S.) in the very high energy (VHE) domain. HESS J1641−463 remained unnoticed by the usual analysis techniques due to confusion with the bright nearby source HESS J1640−465. It emerged at a significance level of 8.5 standard deviations after restricting the analysis to events with energies above 4 TeV. It shows a moderate flux level of $\phi\,(E > 1\,\mathrm{TeV}) = (3.64 \pm 0.44_{\mathrm{stat}} \pm 0.73_{\mathrm{sys}}) \times 10^{-13}\,\mathrm{cm}^{-2}\,\mathrm{s}^{-1}$, corresponding to 1.8% of the Crab Nebula flux above the same energy, and a hard spectrum with a photon index of $\Gamma = 2.07 \pm 0.11_{\mathrm{stat}} \pm 0.20_{\mathrm{sys}}$. It is a point-like source, although an extension up to a Gaussian width of $\sigma = 3$ arcmin cannot be discounted due to uncertainties in the H.E.S.S. point-spread function. The VHE γ-ray flux of HESS J1641−463 is found to be constant over the observed period when checking time binnings from the year-by-year to the 28 minute exposure timescales. HESS J1641−463 is positionally coincident with the radio supernova remnant SNR G338.5+0.1. No X-ray candidate stands out as a clear association; however, *Chandra* and XMM-*Newton* data reveal some potential weak counterparts. Various VHE γ-ray production scenarios are discussed. If the emission from HESS J1641−463 is produced by cosmic ray protons colliding with the ambient gas, then their spectrum must extend close to 1 PeV. This object may represent a source population contributing significantly to the galactic cosmic ray flux around the knee.

Key words: cosmic rays – gamma rays: general – ISM: individual objects (SNR G338.3−0.0, SNR G338.5+0.1)

Online-only material: color figures

1. INTRODUCTION

The large field of view (FoV) of the High Energy Stereoscopic System (H.E.S.S.), together with its stereoscopic observation strategy, allowed the discovery of tens of very high energy (VHE, $\geqslant 0.1$ TeV) γ-ray sources[44] by scanning a large fraction of the Galactic plane (Aharonian et al. 2005a; Carrigan et al. 2013). With deeper exposures, more VHE γ-ray sources are detected, although source confusion begins to be problematic. Complementing the spatial search for new sources, an investigation into energy bands can provide an additional powerful tool for new discoveries. In this work, it will be shown how this method allowed for the detection of a new object, HESS J1641−463 (hereafter J1641−463), previously hidden in the tails of the much brighter object HESS J1640−465. Interestingly, the newly discovered source exhibits one of the hardest spectra observed in VHE γ-rays, allowing its detection at higher energies, where the two sources are clearly separated. Hereafter, the observations and the analysis technique that led to the discovery of J1641−463 are described. Finally, a discussion of plausible counterparts of this source at other wavelengths is presented.

2. H.E.S.S. OBSERVATIONS AND RESULTS

H.E.S.S. is an array of five imaging atmospheric Cherenkov telescopes located in the Khomas Highland of Namibia, 1800 m above sea level. In the initial phase of the H.E.S.S. project, during which the data described here were taken, the array was composed of four 13 m diameter telescopes. Extensive air showers are measured with an average energy resolution of 15% and an angular resolution better than $0.^{\circ}1$ (Aharonian et al. 2006) for a typical energy of 1 TeV. The trigger energy threshold is about 100 GeV and increases with higher zenith angle (Funk et al. 2004).

J1641−463 remained unnoticed by the standard source detection techniques due to its low brightness and its proximity to the bright source HESS J1640−465 (Abramowski et al. 2014). During a study of a possible energy-dependent morphology of HESS J1640−465, a collection of images for events with energies above a set of energy thresholds ($E > 1$, 2, 3, 4, and 5 TeV) was created. J1641−463 was not visible in the original images of the HESS J1640−465 FoV, as those images included no energy cut in the events, and thus were dominated by the much more numerous low-energy events coming from the brighter HESS J1640−465. Thanks to the improved H.E.S.S. point-spread function (PSF) at higher energies and to its hard spectrum, J1641−463 was clearly visible in the highest energy sky maps, where the contamination from HESS J1640−465 was low. This discovery triggered further H.E.S.S. observations, allowing the firm establishment of a new VHE γ-ray source. The VHE γ-ray excess image obtained for $E > 4$ TeV is shown in

[41] Current address: Harvard-Smithsonian Center for Astrophysics, 60 Garden Street, MS-20, Cambridge, MA 02138, USA.
[42] Current address: Santa Cruz Institute for Particle Physics, Department of Physics, University of California at Santa Cruz, Santa Cruz, CA 95064, USA.
[43] Wallenberg Academy Fellow.
[44] See http://tevcat.uchicago.edu/ for an updated list of VHE γ-ray sources.

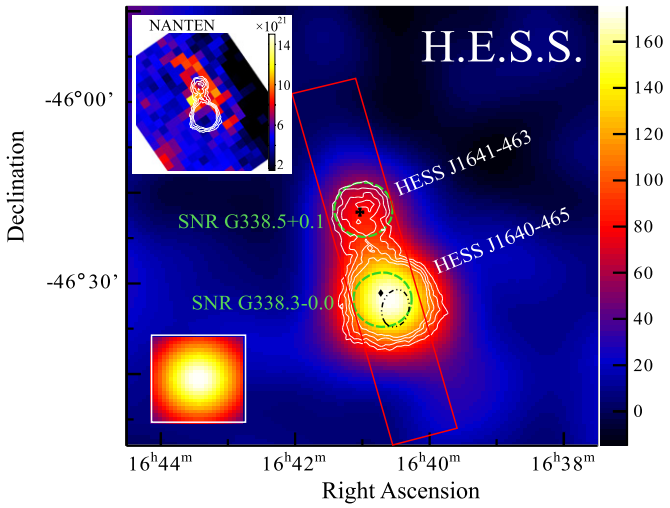

Figure 1. Map of excess events with energies E > 4 TeV for the region around J1641−463 smoothed with a Gaussian of width 0.°085, corresponding to the 68% containment radius of the instrument PSF. The white contours indicate the significance of the emission at the 5, 6, 7, and 8σ level. The black cross indicates the value and uncertainty of the best fit position of the source, the green dashed circles show the positions and approximate extensions of the two nearby SNRs, the black diamond the position of PSR J1640−4631, the dash–dotted black ellipse the 95% confidence error position of 1FHL J1640.54634, and the red box indicates the area for the extraction of the profiles shown in Figure 2. The color scale is in units of counts per smoothing Gaussian width. The H.E.S.S. PSF is shown inside the white box. The upper left inset shows a map of the distribution of the column density of molecular hydrogen in units of cm^{-2}, estimated from the NANTEN CO(1−0) data, together with the H.E.S.S. significance contours.

(A color version of this figure is available in the online journal.)

Figure 1, where the background level is estimated following the ring background model (Berge et al. 2007).

The observations of the FoV around J1641−463 were carried out from 2004 to 2011, corresponding to an acceptance-corrected live time of 72 hr, after quality selection criteria were applied as in Aharonian et al. (2006). The data were analyzed with the methods described in Aharonian et al. (2006).[45] The events were reconstructed using the Hillas parameter technique (Hillas 1995). The results were cross-checked using two independent analysis methods (Ohm et al. 2009; de Naurois & Rolland 2009).

The position of J1641−463 (together with the nearby HESS J1640−465) was determined by fitting a two-dimensional double-Gaussian model convolved with the H.E.S.S. PSF to the two-dimensional ON-source excess event distribution for $E > 4$ TeV, energies at which source confusion with HESS J1640−465 is mitigated. The centroid of the Gaussian corresponding to the location of J1641−463 was found to be $\alpha_{J2000} = 16^h41^m2.^s1 \pm 3.^s0_{stat} \pm 1.^s9_{sys}$, $\delta_{J2000} = -46°18'13'' \pm 35''_{stat} \pm 20''_{sys}$. The source is found to be point-like, but a slightly extended morphology up to a width of $\sigma = 3$ arcmin cannot be ruled out due to uncertainties in the H.E.S.S. PSF.

Figure 2 shows the projection of the excess events in the rectangular region shown in Figure 1 for different energy bands. An F-test (Martin 1971) was performed comparing the single Gaussian model fits with the double-Gaussian fits. For all the energy bands, the null hypothesis can be rejected at significance levels of 3.6–4.3σ, thus clearly favoring the double-Gaussian model.

[45] The H.E.S.S. hap-12-03 analysis software package with version 32 instrument response tables was used.

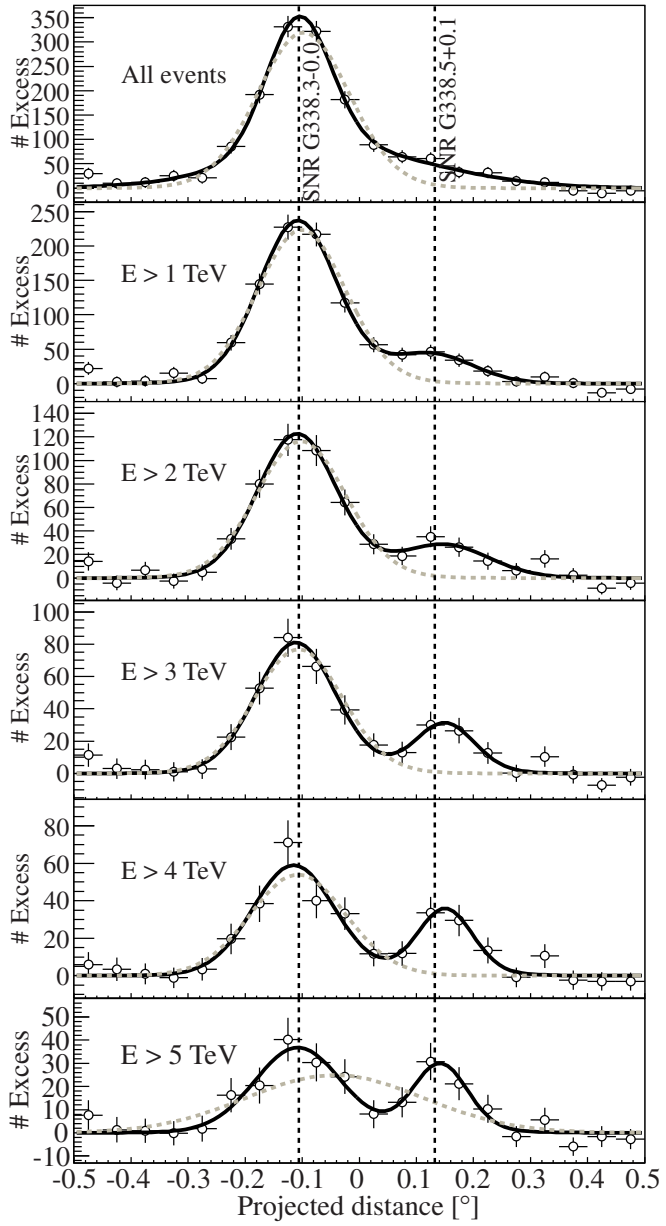

Figure 2. Distribution of VHE γ-ray excess profiles and Gaussian fits (convolved with the instrument PSF) for the red rectangular slice shown in Figure 1. Vertical lines show the position of the SNR 338.3−0.0 and G338.5+0.1. Fits using a single and a double Gaussian function are shown in dashed and solid lines, respectively. Note that the energy dependence of the PSF is taken into account in the fits.

In order to minimize the contamination from HESS J1640−465, hard cuts were used, which imply a cut on θ^2 (the square of the angular difference between the reconstructed shower direction and the source position) of 0.01 deg^2, and on the individual image charge in photo-electrons of 200. The source is detected with a statistical significance of 8.5σ above 4 TeV, determined by using Equation (17) in Li & Ma (1983) after background suppression with the reflected background model (Berge et al. 2007).

The differential VHE γ-ray spectrum of J1641−463, derived using the forward-folding technique (Piron et al. 2001), is compatible with a power-law function $dN/dE = \phi_0 \times (E/1\,\mathrm{TeV})^{-\Gamma}$ with $\phi_0 = (3.91 \pm 0.69_{stat} \pm 0.78_{sys}) \times 10^{-13}\,\mathrm{cm^{-2}\,s^{-1}\,TeV^{-1}}$ and $\Gamma = 2.07 \pm 0.11_{stat} \pm 0.20_{sys}$ for the energy range from 0.64 to 100 TeV. The flux level is $\phi(E > 1\,\mathrm{TeV}) = (3.64 \pm$

$0.44_{\rm stat} \pm 0.73_{\rm sys}) \times 10^{-13}\,{\rm cm}^{-2}\,{\rm s}^{-1}$, corresponding to 1.8% of the Crab Nebula flux above the same energy. At those energies, the estimated total contamination from HESS J1640−465 is 15 ± 6%, reduced at higher energies (4 ± 3% at $E > 4$ TeV). A fit by a power law with an exponential cutoff is not statistically justified given the low flux level of J1641−463. A fit to a constant value of the period-by-period[46] light curve for energies above 0.64 TeV yields a $\chi^2/{\rm d.o.f.} = 11.7/14$, with a p-value of 63%. No variability can be seen in other time binnings (from year-by-year to 28 minute exposures).

3. SEARCH FOR COUNTERPARTS AT OTHER WAVELENGTHS

3.1. Radio Observations

J1641−463 is found within the bounds of SNR G338.5+0.1 (Green 2009). This supernova remnant (SNR) is located at $\alpha_{J2000} = 16^{\rm h}40^{\rm m}59^{\rm s}$, $\delta_{J2000} = -46^\circ17'.8$, has a roughly circular morphology, and shows a flux density at 1 GHz of ≈ 12 Jy (Green 2009). A diameter between 5′ (the most obvious non-thermal emission region reported in Whiteoak & Green 1996) to 9′ (Green 2009) for G338.5+0.1 is assumed in this work, and the latter is displayed in Figure 1. Kothes & Dougherty (2007) conclude that the source is located at a distance of 11 kpc,[47] which implies a physical size between ≈ 16 to ≈ 30 pc. Assuming that G338.5+0.1 is in the Sedov–Taylor phase, the Sedov solution (see, e.g., van der Swaluw 2001) is used to estimate its age; with an explosion energy of 10^{51} erg and the density of the external medium between 0.1 and 1 cm^{-3}, the age of the SNR would correspond to 1.1−3.5 kyr and 5−17 kyr for 16 pc and 30 pc diameter, respectively.

The distribution of molecular gas around J1641−463 is shown in the top left inset of Figure 1. This distribution is obtained by integrating the CO 1→0 rotational line emission, measured with NANTEN, over a range in velocity between −40 km s^{-1} and −30 km s^{-1} (Matsunaga et al. 2001; Mizuno & Fukui 2004). The choice of this range is motivated by the presence of dense molecular cloud clumps in the region, mapped with various NH_3 emission lines with the MOPRA survey at those velocities (de Wilt et al. 2012). Using the model for the Galactic rotation curves by Kothes & Dougherty (2007), we can determine that the gas is located at a distance of about 11 kpc.

Assuming a ratio $X_{\rm CO->N_{H_2}} = 1.5 \times 10^{20}$ between the CO velocity integrated intensity and the column density of molecular gas, N_{H_2}, the total column density from the extraction region of J1641−463 is 1.7×10^{22} cm^{-2}. At 11 kpc, the density and the total mass are about 100 cm^{-3} and 2.4×10^5 solar masses, respectively.

3.2. X-Ray Observations

No candidate for an X-ray counterpart of J1641−463 was found in existing catalogs, even when extending the search radius to 0.°1 away from the source. Two data sets from *Chandra* and one from XMM-*Newton* were thus inspected in order to search for an X-ray counterpart of J1641−463.

The *Chandra* ObsID 11008 partially covers J1641−463, with 40 ks of exposure, while ObsID 12508 fully encloses it with 19 ks. The data sets were processed with the CIAO package.

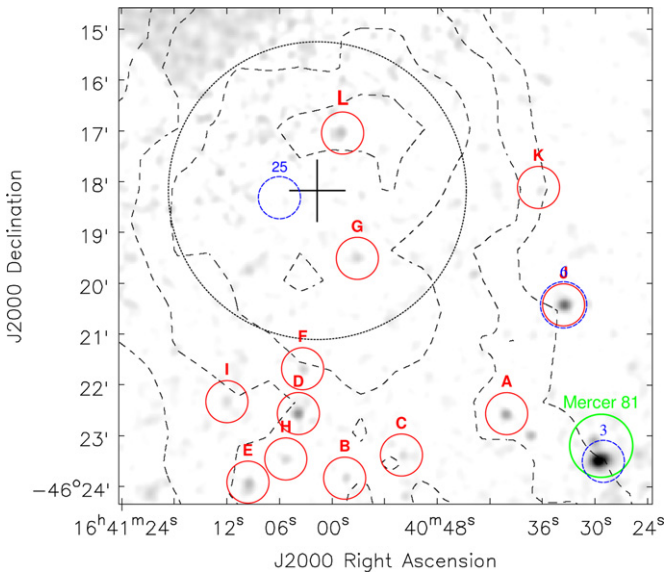

Figure 3. *Chandra* [1.0−10 keV] mosaic image of the field surrounding J1641−463 from the ObsIDs 11008 and 12508. The image was exposure-corrected, background subtracted, and smoothed with a Gaussian of width 10″. The best-fit position of J1641−463 with 1σ error bars is indicated with the black cross, while the upper limit to the source extension fit is indicated by the surrounding black circle. The detected hard X-ray sources are shown as red circles. The blue dashed circles indicate the positions of the sources detected using XMM-*Newton* data. The dashed contours indicate the significance of the VHE γ-ray emission as shown in Figure 1. The thick green circle shows the position of the stellar cluster Mercer 81, the target of the ObsID 11008.

(A color version of this figure is available in the online journal.)

The tool `wavdetect` was used to identify sources, providing 32 faint point-like or marginally extended candidates at distances smaller than 0.°1 to the J1641−463 position. This sample was filtered by 2 criteria, reducing the sample to 12 candidates (see Figure 3): first, the sources with signal-to-noise ratios below 3 were rejected. Second, a cut on the hardness ratio as defined in Elvis et al. (2009) was applied, HR = $(H-S)/(H+S)$, where H are the counts with 2−10 keV and S the counts with 0.3−2 keV. The sources with HR ⩽ 0 were excluded. Spectral fits using an absorbed power-law model were performed assuming a value of N_H of 2.0×10^{22} cm^{-2}, corresponding to the values reported by Kalberla et al. (2005) and Dickey & Lockman (1990), in good agreement with those derived with the NANTEN data. The estimated flux densities in the 0.3−10 keV energy band result in values from 7×10^{-15} erg cm^{-2}s^{-1} (src. B) to 1.5×10^{-13}erg cm^{-2} s^{-1} (src. L). No evidence of variability was found for any of the sources after performing a one-sample Kolmogorov–Smirnov test: the probability $P_{\rm KS}$ for the hypothesis of a uniform flux was $P_{\rm KS} > 0.1$. None these sources is an obvious counterpart of J1641−463 due to their low fluxes and the lack of any morphological feature that could point to such an association.

The *XMM-Newton* ObsID 0302560201, covering the region of HESS J1640−465 (Funk et al. 2007), constitutes a partial 23.7 ks exposure of the source area. The data set was analyzed using the XMM SAS analysis task `edetect_chain` simultaneously in all three cameras and the five standard energy bands. In this manner, 27 sources were found, with only one consistent with the position and upper limit to the extension of J1641−463 (see Figure 3). This source was detected only in the pn camera and only in the energy band 0.5−1 keV with a significance of ≈4.6σ, and it is not detected in the *Chandra* data. The vignetting for this source is 0.35 in the pn camera, so the observation is

[46] A H.E.S.S. observing period is the period between two full moons.

[47] Although Shaver & Goss (1970) report a closer distance of 5.3 kpc, in this work it is assumed at a distance of 11 kpc as reported by Kothes & Dougherty (2007).

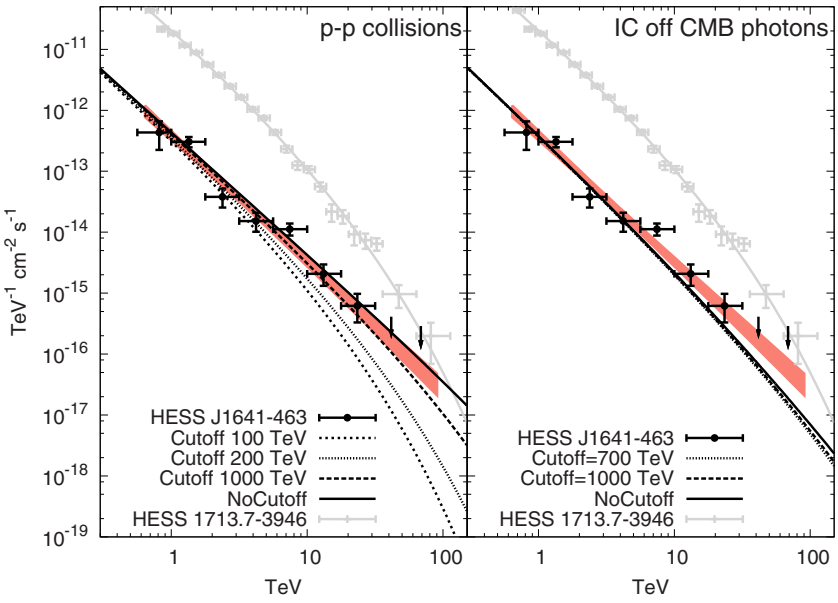

Figure 4. Differential γ-ray spectrum of J1641−463, together with the expected emission from p–p collisions (left) and IC off CMB photons (right). The pink area represents the 1σ confidence region for the fit to a power-law model, the black data points the H.E.S.S. measured photon flux (1σ uncertainties), the arrows the 95% CL upper limits on the flux level, and the black curves the expected emission from the models, assuming different particle energy cutoff values. For comparison, the gray data points and curve represent the archival spectrum and the corresponding best-fit model, respectively, of SNR RX J1713.7−3946 (Aharonian et al. 2007).

(A color version of this figure is available in the online journal.)

very insensitive to the region of interest. Due to low statistics, calculating an HR or spectrum for this source was not possible, and it is unclear whether this may represent a counterpart.

3.3. HE Observations

The only High Energy (HE, 0.1−100 GeV) source found within 0.°5 of J1641−463 is 2FGL J1640.5−4633 (Nolan et al. 2012), also present in the 10 > GeV *Fermi*/Large Area Telescope (LAT) Catalog as 1FHL J1640.5−4634 (Ackermann et al. 2013), likely to be associated with HESS J1640−465 (Slane et al. 2010; Gotthelf et al. 2014; see Figure 1). If the spectrum of J1641−463 is extended to lower energies as a featureless power law, its HE counterpart could be confused with 1FHL J1640.54634. However, the extrapolation of the VHE emission of J1641−463 to the *Fermi*/LAT energy ranges predicts a flux of $(5.0 \pm 2.8) \times 10^{-11}$ cm^{-2} s^{-1} in the 10−500 GeV band, a factor 10 lower than the flux of 1FHL J1640.5−4634 at those energies, and thus a detection of a GeV excess on the position of J1641−463 would imply either a contribution from an unrelated source or from a different component of radiation of the same source. A study to resolve such a faint, confused source is challenging and outside the scope of this work.

4. DISCUSSION

Possible scenarios to explain the emission from J1641−463 include the emission from accelerated particles within an SNR, a molecular cloud illuminated by cosmic rays (CRs), a pulsar wind nebula (PWN), and a γ-ray binary. These scenarios are discussed below.

If G338.5+0.1 is a young SNR, it can accelerate particles up to hundreds of TeV. The left panel of Figure 4 shows the comparison between the H.E.S.S. spectrum and the spectrum produced by accelerated protons from G338.5+0.1 interacting with the ambient gas. The predicted spectra are calculated using the parameterization of Kelner et al. (2006), assuming a proton spectrum with a power-law slope of −2.1 and multiple cutoff energies. The profile of the log-likelihood ratio test statistic (Rolke et al. 2005) was used to estimate a confidence interval of the cutoff energies, while considering the spectral index and normalization as nuisance parameters and ignoring systematic errors. The 99% confidence level (CL) lower limit on the cutoff energy corresponds to 100 TeV. This proton spectrum is one of the hardest ever inferred to explain the emission from a γ-ray source and agrees well with the prediction by diffusive shock acceleration in young SNRs. Remarkably, the γ-ray spectrum of J1641−463 is harder than that observed from the young SNR RXJ1713−4936 at energies above few TeV, where a cutoff is seen (Aharonian et al. 2007). If the TeV luminosity measured by H.E.S.S. is produced by collisions of protons with the ambient gas, then the total energy of the supernova explosion converted into hadron acceleration is $W_p = L_\gamma\, t_{\pi^0}, \approx 10^{50} n^{-1}$, where $L_\gamma = 4 \times 10^{34}$ erg s^{-1} is the total luminosity measured by H.E.S.S. above 0.64 TeV (at 11 kpc) and $t_{\pi^0} \approx 5 \times 10^{15} (n/1\,\mathrm{cm}^{-3})^{-1}$ s is the cooling time of protons through the channel of π^0 production (Aharonian 2004). With a proton spectrum extending almost up to 1 PeV, J1641−463 may represent a source population contributing significantly to the galactic CR flux around the knee.

If G338.5+0.1 is older (5−17 kyr; see Section 3.1), then VHE protons accelerated by the young SNR G338.3−0.0, positionally coincident with HESS J1640−465 (Abramowski et al. 2014), could have already reached the dense molecular cloud (MC) coincident with J1641−463. This would explain the relatively high brightness of J1641−463 in comparison with HESS J1640−465 at high energies, as shown in Figure 2 (Aharonian & Atoyan 1996; Gabici et al. 2009). In such a scenario, HESS J1640−465 would no longer look like a *pevatron*, as the highest energy CRs would have already left (Aharonian & Atoyan 1996). The much younger adjacent G338.3−0.0 would be in this scenario a major source of CRs.

Electrons of hundreds of TeV IC (inverse Compton) scattering off the cosmic microwave background photons (CMB)

could explain the emission from J1641−463. These electrons would be accelerated either in G338.5+0.1 or in the PWN associated with the young energetic pulsar, PSR J1640−4631, discovered within the observational boundaries of HESS J1640−465 (Gotthelf et al. 2014). Even assuming a pure power law for the primary electron spectrum, the cross section for IC scattering decreases at high energies resulting in a break in the γ-ray spectrum at multi TeV energies. Such a break is not observed in the spectrum of J1641−463. The predicted IC radiation, shown in the right panel of Figure 4, was obtained by assuming that the electron cooled spectrum is a power law of spectral index −3.14 with different cutoff energies. The 99% CL lower limit on the cutoff energy, derived as in the case of the proton model using the exact Klein–Nishina expression for the IC emission, corresponds to 700 TeV. It is extremely difficult to accelerate electrons in SNRs to such energies, as hundred TeV electrons suffer severe synchrotron losses in the amplified magnetic fields of acceleration sites. Both the absence of a break in the γ-ray spectrum of J1641−463 and the derived lower limit on the cutoff energy of the electron spectrum strongly disfavor the leptonic scenario.

A γ-ray binary scenario could also be considered, given the point-like morphology of J1641−463 and that a similarly hard spectral index of −2.23 has been found in one of these systems (LS 5039; Aharonian et al. 2005b). An X-ray flux as low as $\sim 10^{-14}$ erg cm^{-2} s^{-1} is expected from a faint X-ray binary system similar to HESS J0632+057 (Hinton et al. 2009) assuming a distance of 11 kpc, where the lack of an obvious optical counterpart could be due to high optical extinction caused by the large distance and the position close to the Galactic plane.

5. CONCLUSIONS

Deeper exposures with H.E.S.S. together with a study of the emission in various energy bands made it possible to discover a new unique VHE source, showing one of the hardest γ-ray spectra ever found at these energies, extending up to at least 20 TeV without a break. In order to explain the observed VHE γ-ray spectrum, scenarios where protons are accelerated up to hundreds of TeV at either G338.5+0.1 or G338.3−0.0 and then interact with local gas or nearby massive MCs are the most compelling ones. Other possible scenarios, such as a PWN or a γ-ray binary, are disfavored but cannot be discarded. Deeper X-ray and VHE γ-ray observations, together with a better PSF for the latter, would allow for a better identification of the source.

The support of the Namibian authorities and of the University of Namibia in facilitating the construction and operation of H.E.S.S. is gratefully acknowledged, as is the support by the German Ministry for Education and Research (BMBF), the Max Planck Society, the French Ministry for Research, the CNRS-IN2P3, and the Astroparticle Interdisciplinary Programme of the CNRS, the U.K. Science and Technology Facilities Council (STFC), the IPNP of the Charles University, the Polish Ministry of Science and Higher Education, the South African Department of Science and Technology and National Research Foundation, and by the University of Namibia. We appreciate the excellent work of the technical support staff in Berlin, Durham, Hamburg, Heidelberg, Palaiseau, Paris, Saclay, and in Namibia in the construction and operation of the equipment. This research has made use of *Chandra* Archival data, as well as the *Chandra* Source Catalog, provided by the *Chandra* X-ray Center (CXC) as part of the *Chandra* Data Archive. This research has made use of software provided by the *Chandra* X-ray Center (CXC) in the application packages CIAO, ChIPS, and Sherpa. This research uses observations obtained with XMM-*Newton*, an ESA science mission with instruments and contributions directly funded by ESA Member States and NASA. This research has made use of the SIMBAD database, operated at CDS, Strasbourg, France. The work of J.M. was funded by contract ERC-StG-259391 from the European Community.

Facility: H.E.S.S.

REFERENCES

Abramowski, A., Aharonian, F., Benkhali, F. A., et al. 2014, MNRAS, 439, 2828
Ackermann, M., Ajello, M., Allafort, A., et al. 2013, ApJS, 209, 34
Aharonian, F. A. 2004, Very High Energy Cosmic Gamma Radiation: A Crucial Window on the Extreme Universe (River Edge, NJ: World Scientific Publishing)
Aharonian, F. A., Akhperjanian, A. G., Aye, K.-M., et al. 2005a, Sci, 307, 1938
Aharonian, F. A., Akhperjanian, A. G., Aye, K.-M., et al. 2005b, Sci, 309, 746
Aharonian, F. A., Akhperjanian, A. G., Bazer-Bachi, A. R., et al. 2006, A&A, 457, 899
Aharonian, F. A., Akhperjanian, A. G., Bazer-Bachi, A. R., et al. 2007, A&A, 464, 235
Aharonian, F. A., & Atoyan, A. M. 1996, A&A, 309, 917
Berge, D., Funk, S., & Hinton, J. 2007, A&A, 466, 1219
Carrigan, S., Brun, F., Chaves, R. C. G., et al. 2013, arXiv:1307.4690
de Naurois, M., & Rolland, L. 2009, APh, 32, 231
de Wilt, P., Rowell, G., Dawson, B., et al. 2012, in AIP Conf. Ser. 1505, 5th Heidelberg Internatiional Symposium on High-Energy Gamma-Ray Astronomy, ed. F. A. Aharonian, W. Hofmann, & F. M. Rieger (Melville, NY: AIP), 277
Dickey, J. M., & Lockman, F. J. 1990, ARA&A, 28, 215
Elvis, M., Civano, F., Vignali, C., et al. 2009, ApJS, 184, 158
Funk, S., Hermann, G., Hinton, J., et al. 2004, APh, 22, 285
Funk, S., Hinton, J. A., Pühlhofer, G., et al. 2007, ApJ, 662, 517
Gabici, S., Aharonian, F. A., & Casanova, S. 2009, MNRAS, 396, 1629
Gotthelf, E. V., Tomsick, J. A., Halpern, J. P., et al. 2014, ApJ, 788, 155
Green, D. A. 2009, BASI, 37, 45
Hillas, A. M. 1985, Proc. of the 19th ICRC (La Jolla), 3, 445
Hinton, J. A., Skilton, J. L., Funk, S., et al. 2009, ApJL, 690, L101
Kalberla, P. M. W., Burton, W. B., Hartmann, D., et al. 2005, A&A, 440, 775
Kelner, S. R., Aharonian, F. A., & Bugayov, V. V. 2006, PhRvD, 74, 034018
Kothes, R., & Dougherty, S. M. 2007, A&A, 468, 993
Li, T.-P., & Ma, Y.-Q. 1983, ApJ, 272, 317
Martin, B. R. 1971, Statistics for Physicists (New York: Academic Press)
Matsunaga, K., Mizuno, N., Moriguchi, Y., et al. 2001, PASJ, 53, 1003
Mizuno, A., & Fukui, Y. 2004, in ASP Conf. Ser. 317, Milky Way Surveys: The Structure and Evolution of our Galaxy, ed. D. Clemens, R. Shah, & T. Brainerd (San Francisco, CA: ASP), 59
Nolan, P. L., Abdo, A. A., Ackermann, M., et al. 2012, ApJS, 199, 31
Ohm, S., van Eldik, C., & Egberts, K. 2009, APh, 31, 383
Piron, F., Djannati-Atai, A., Punch, M., et al. 2001, A&A, 374, 895
Rolke, W. A., López, A. M., & Conrad, J. 2005, NIMPA, 551, 493
Shaver, P. A., & Goss, W. M. 1970, AuJPA, 14, 133
Slane, P., Castro, D., Funk, S., et al. 2010, ApJ, 720, 266
van der Swaluw, E. 2001, PhD thesis, Utrecht Univ.
Whiteoak, J. B. Z., & Green, A. J. 1996, A&AS, 118, 329